Science Advances
AAAS

advances.sciencemag.org/cgi/content/full/5/5/eaav7116/DC1

Supplementary Materials for

Defining early SIV replication and dissemination dynamics following vaginal transmission

Claire Deleage, Taina T. Immonen, Christine M. Fennessey, Arnold Reynaldi, Carolyn Reid, Laura Newman, Leslie Lipkey, Timothy E. Schlub, Celine Camus, Sean O'Brien, Jeremy Smedley, Jessica M. Conway, Gregory Q. Del Prete, Miles P. Davenport, Jeffrey D. Lifson, Jacob D. Estes*, Brandon F. Keele*

*Corresponding author. Email: estesja@ohsu.edu (J.D.E.); keelebf@mail.nih.gov (B.F.K.)

Published 29 May 2019, *Sci. Adv.* **5**, eaav7116 (2019)
DOI: 10.1126/sciadv.aav7116

This PDF file includes:

Supplementary Materials

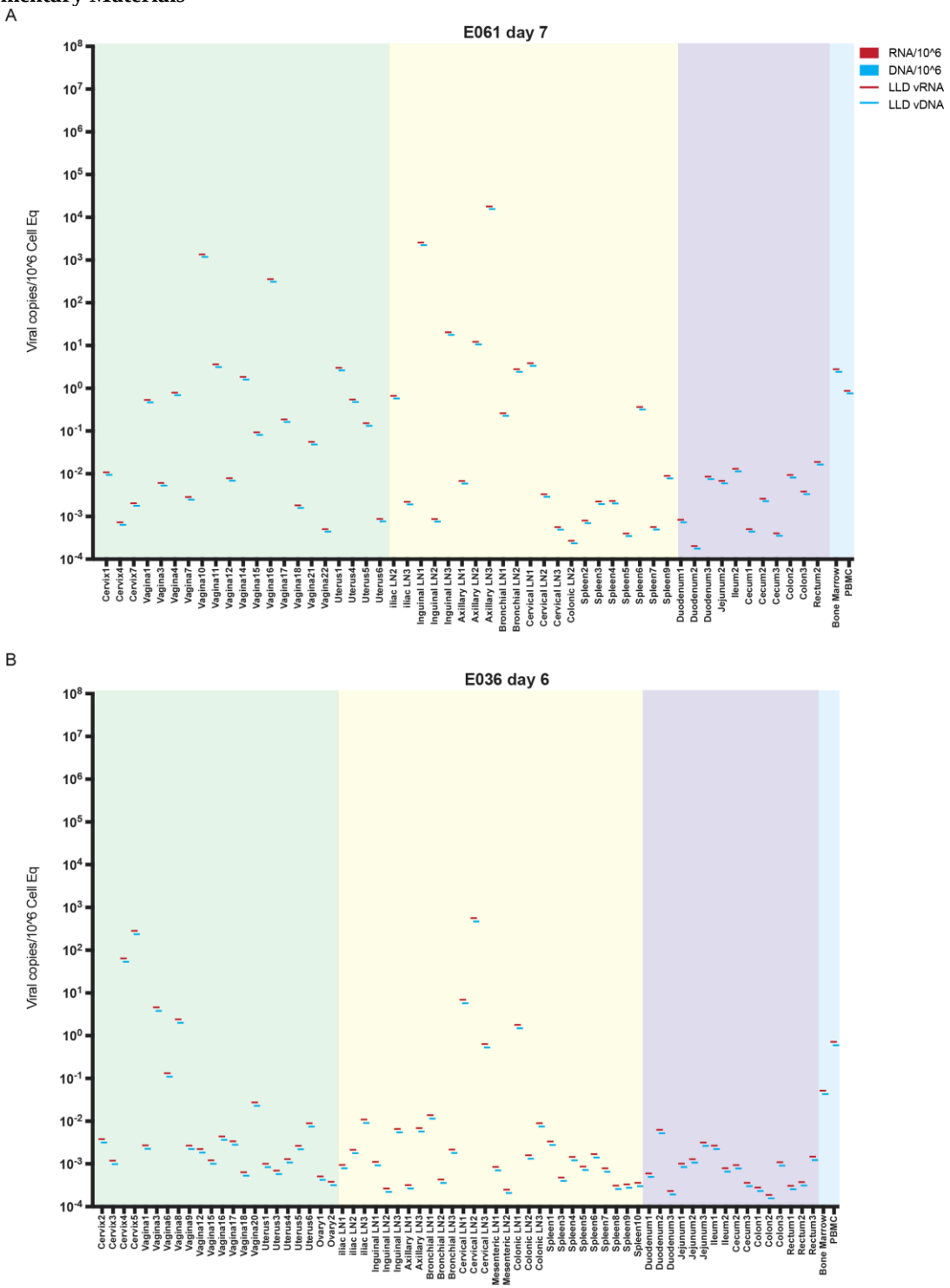

Fig. S1. No viral nucleic acid signal detected in two exposed animals. RNA and DNA were isolated from ~1cm^3 piece of tissue and assayed for viral nucleic acid using qRT-PCR and qPCR. Shading indicates different types of tissues (green: female genital tract, yellow: lymphatic system, purple: GI tract, and blue contains bone marrow and PBMCs). No detectable vRNA or vDNA was measured in animal E061 (A) or E036 (B). The lower limit of detection is estimated as 1 over the total cell equivalence assayed. These detection limits are indicated by a red (vRNA) or blue (vDNA) mark.

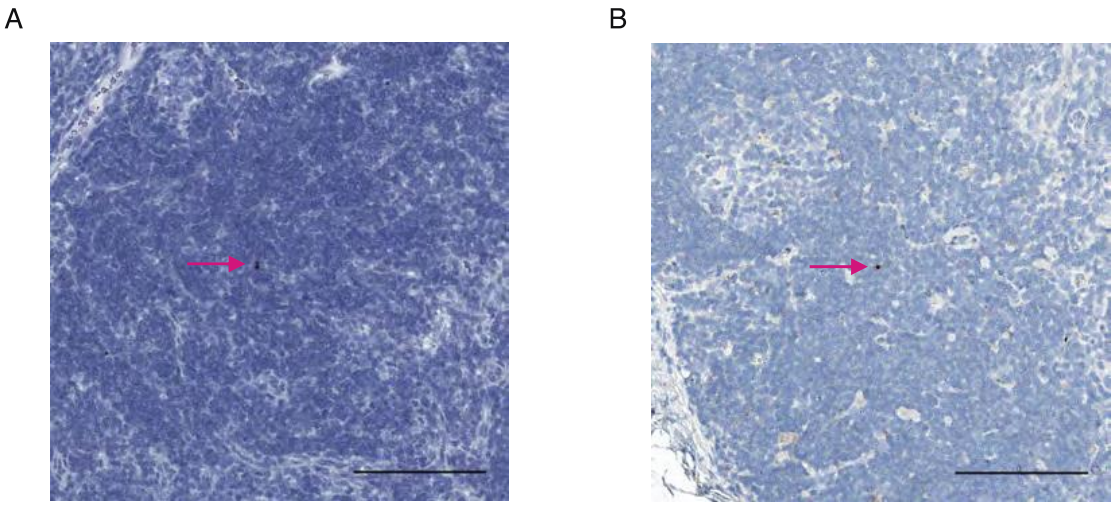

Fig. S2. Detection of rare vRNA- and vDNA-positive cells in draining LN before systemic dissemination. RNAscope was used to identify vRNA positive cells (A) and DNAscope vDNA positive cells (B) in the draining LNs of the PCR negative animal (E061) at day 7 post challenge. Red arrows point to vRNA and vDNA positive cells, which are stained red. Scale bar equals 100µm.

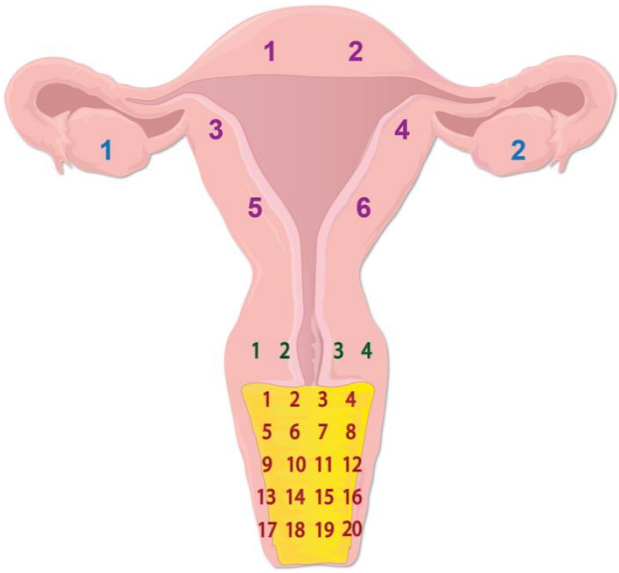

Fig. S3. Schematic representation of FGT tissue collection schema. Individual tissue pieces were collected for nucleic acid analysis or *in situ* analysis according to individually numbered regions in vagina, cervix, uterus, and ovaries.

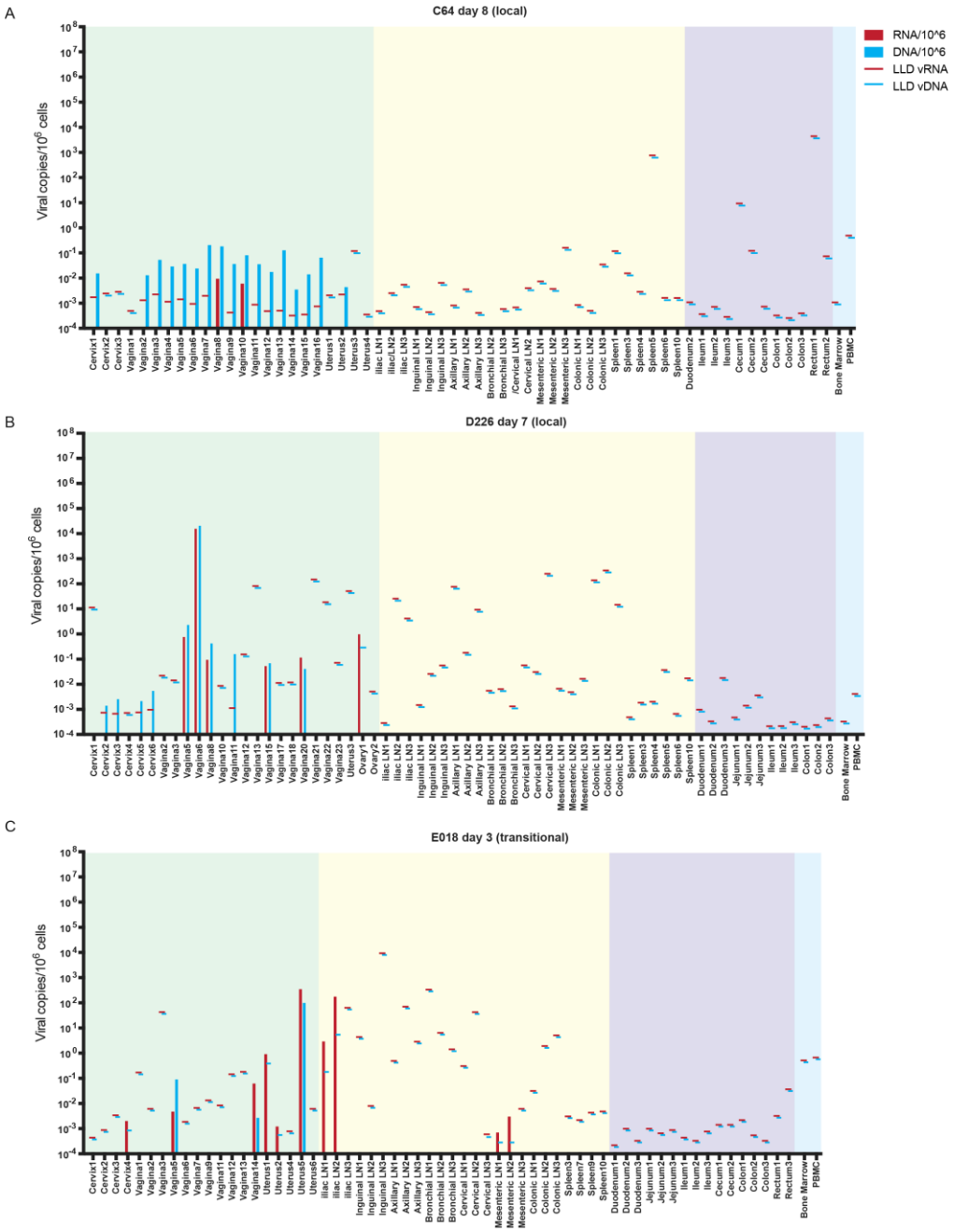

Fig. S4 (A-C). **Viral nucleic acid distribution within individual tissue pieces.** Viral RNA (red) and vDNA (blue) bar graphs indicate viral copies of nucleic acid per million cell equivalences. Each ~1cm^3 piece of tissue was isolated and quantified independently. Shading indicates different types of tissues (green: female genital tract, yellow: lymphatic system, purple: GI tract, and blue contains bone marrow and PBMCs). Animals C64 (A) and D226 (B) represent infection with detectable virus only with the FGT—*local*. Animals E018 (C), E024 (D), E053 (E), and E048 (F) have evidence of productive infection with detectable virus locally as well as within some draining and distal LNs. Animals D290 (G), ELV (H) and E052 (I) represents systemic infection with virus detectable in FGT, LNs/spleen and some GI tract tissues. The lower limit of detection is estimated as 1 over the total cell equivalence assayed. These detection limits are indicated by a red (vRNA) or blue (vDNA) mark.

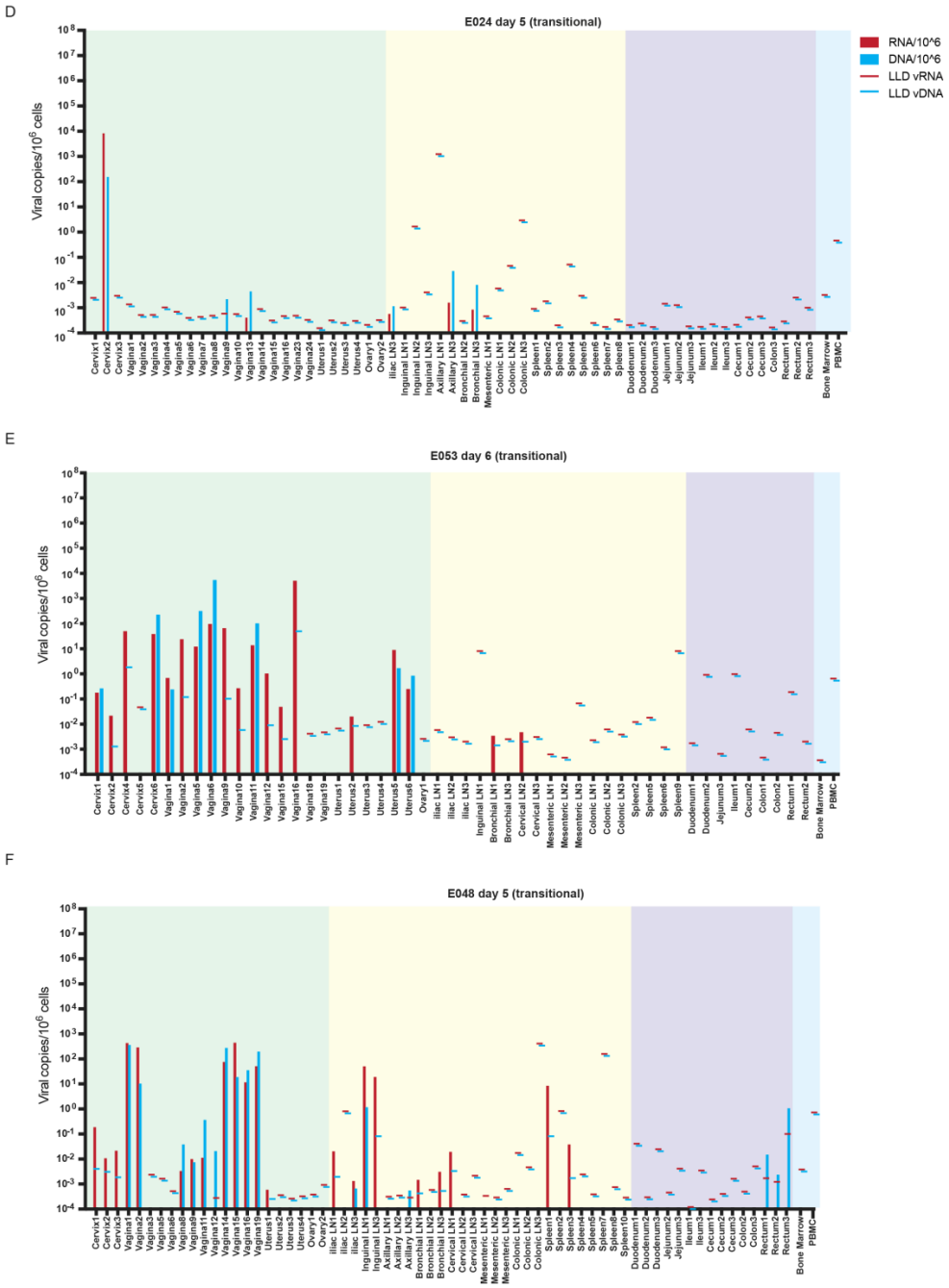

Fig. S4 (D-F). **Viral nucleic acid distribution within individual tissue pieces**. Viral RNA (red) and vDNA (blue) bar graphs indicate viral copies of nucleic acid per million cell equivalences. Each ~1cm^3 piece of tissue was isolated and quantified independently. Shading indicates different types of tissues (green: female genital tract, yellow: lymphatic system, purple: GI tract, and blue contains bone marrow and PBMCs). Animals C64 (A) and D226 (B) represent infection with detectable virus only with the FGT—*local*. Animals E018 (C), E024 (D), E053 (E), and E048 (F) have evidence of productive infection with detectable virus locally as well as within some draining and distal LNs. Animals D290 (G), ELV (H) and E052 (I) represents systemic infection with virus detectable in FGT, LNs/spleen and some GI tract tissues. The lower limit of detection is estimated as 1 over the total cell equivalence assayed. These detection limits are indicated by a red (vRNA) or blue (vDNA) mark.

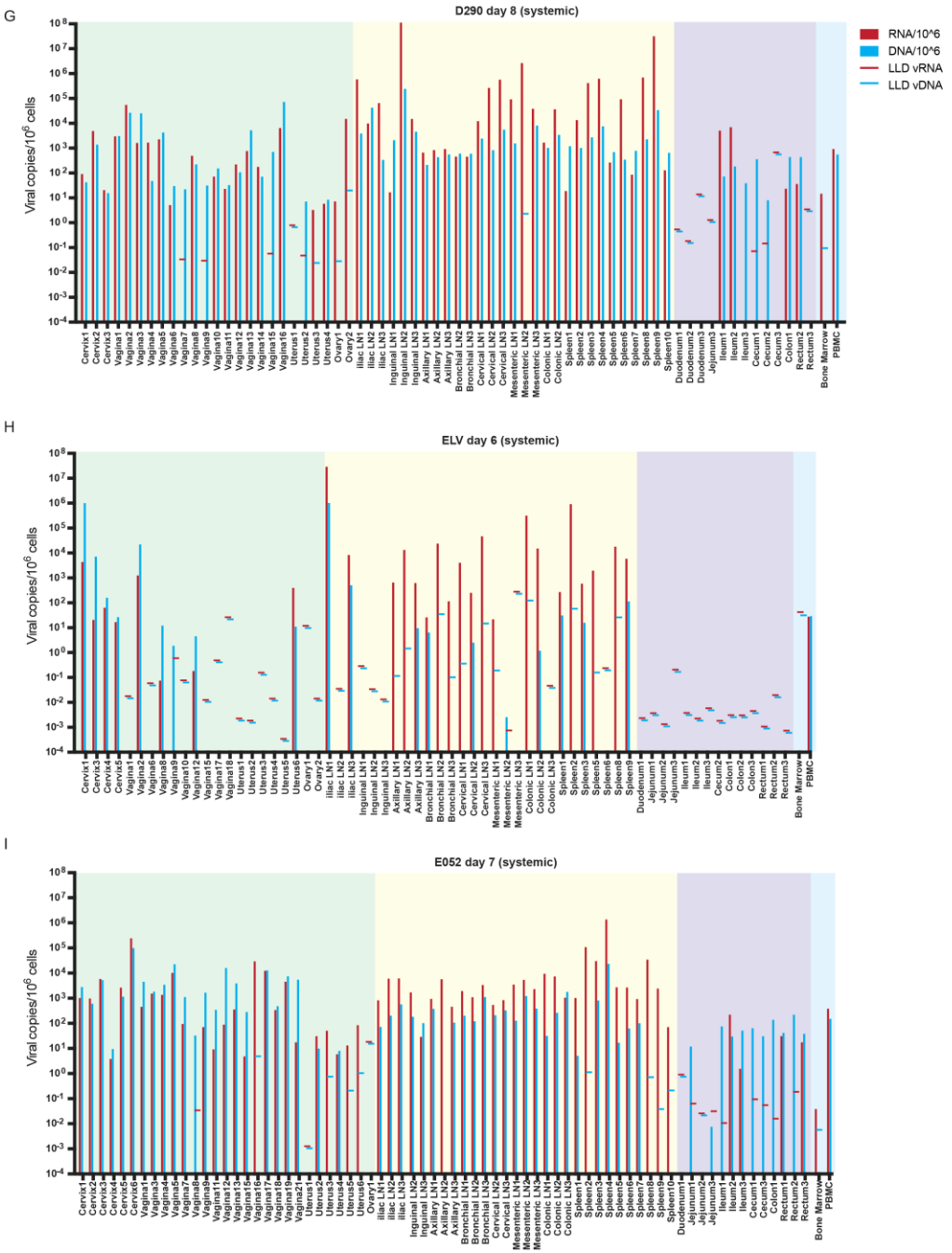

Fig. S4 (G-I). **Viral nucleic acid distribution within individual tissue pieces.** Viral RNA (red) and vDNA (blue) bar graphs indicate viral copies of nucleic acid per million cell equivalences. Each ~1cm^3 piece of tissue was isolated and quantified independently. Shading indicates different types of tissues (green: female genital tract, yellow: lymphatic system, purple: GI tract, and blue contains bone marrow and PBMCs). Animals C64 (A) and D226 (B) represent infection with detectable virus only with the FGT—*local*. Animals E018 (C), E024 (D), E053 (E), and E048 (F) have evidence of productive infection with detectable virus locally as well as within some draining and distal LNs. Animals D290 (G), ELV (H) and E052 (I) represents systemic infection with virus detectable in FGT, LNs/spleen and some GI tract tissues. The lower limit of detection is estimated as 1 over the total cell equivalence assayed. These detection limits are indicated by a red (vRNA) or blue (vDNA) mark.

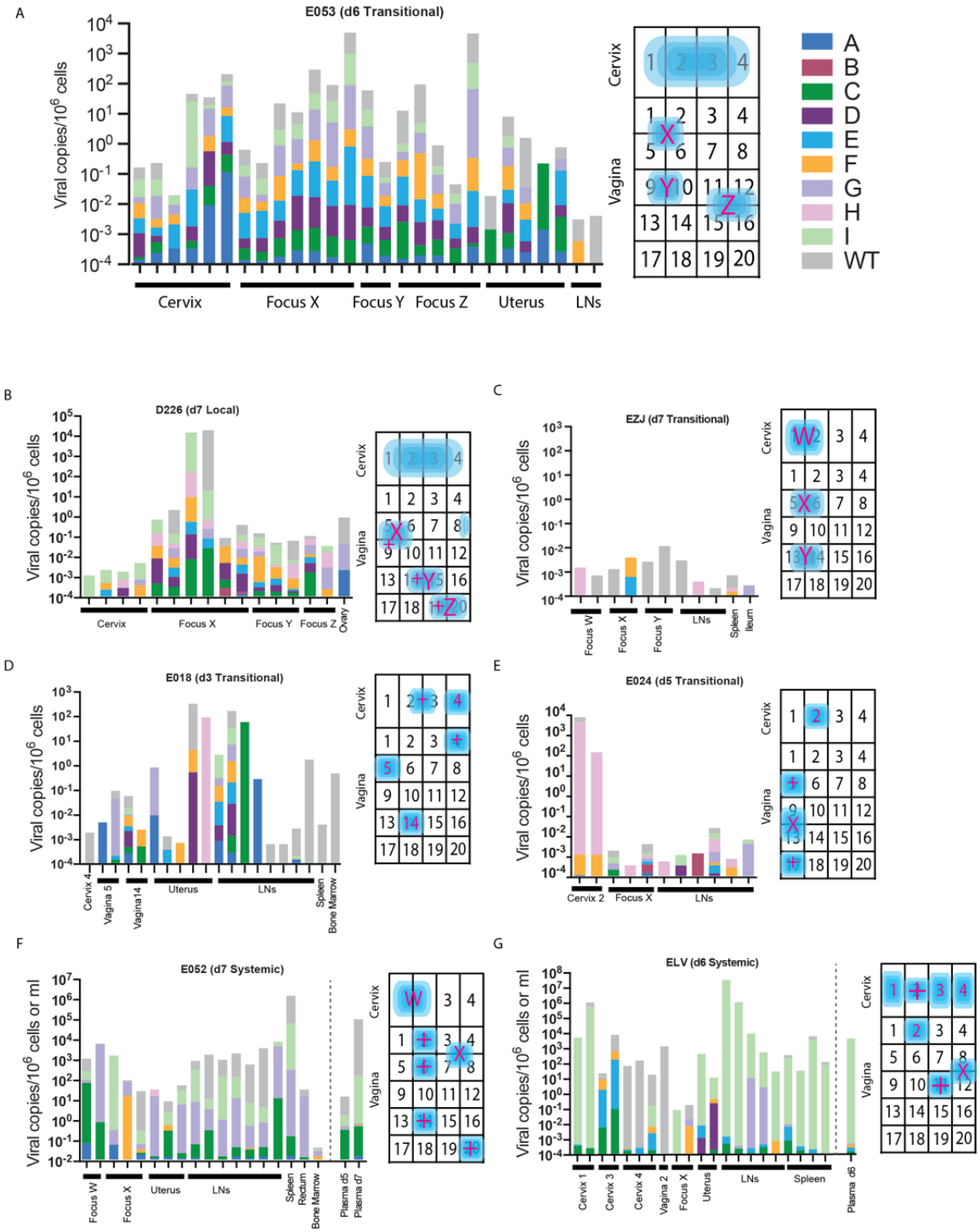

Fig. S5. Proportion and quantification of each variant in virus-positive tissues. For local replication only animal D226 (B), transitional animals E053 (A), EZJ (C), E018 (D), and E024 (E), and the early disseminated animals E052 (F), and ELV (G), all nucleic acid positive tissues are displayed as the height of the bar corresponding to the log-scale on the left axis. The relative proportion of each viral variant is represented by color coding within each bar representing the linear proportion of variants A-WT). Individual foci of infection are indicated schematically within the FGT. In addition to PCR-positive tissue, RNAscope positive sites are indicated (+). Days post infection and infection phase are listed for each panel.

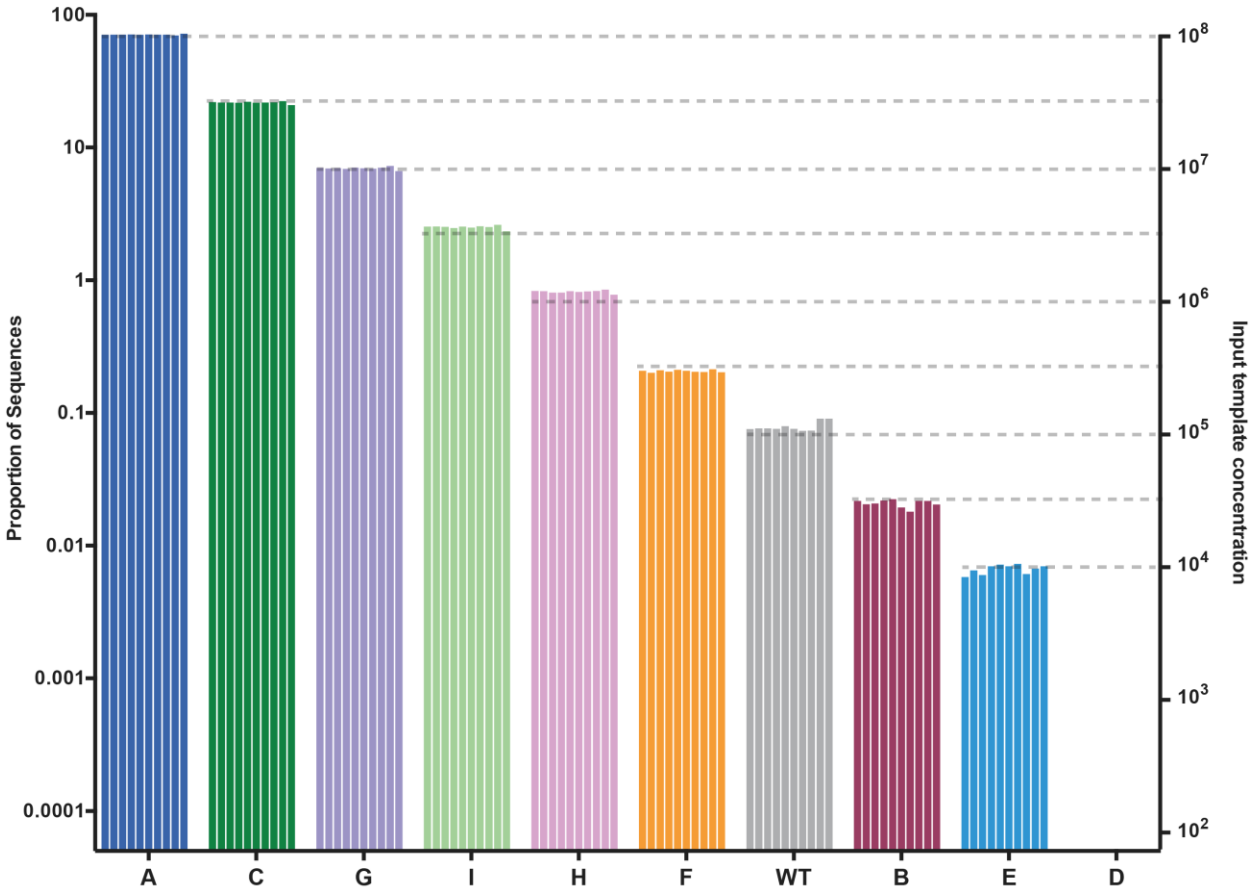

Fig. S6. Proportional representation of sequences following NGS. Nine of the 10 individually tagged viruses were mixed at half log dilutions and vRNA was extracted from this mixture and sequenced across 10 replicates using the MiSeq sequencing protocol. The proportion of each variant was consistent between replicates with concordance between variants across the 4-log dilution range. Variant D was excluded from the dilution series and was found in only 2 of 22 million reads representing a low error rate using this approach (false-positive rate of $<1x10^{-7}$).

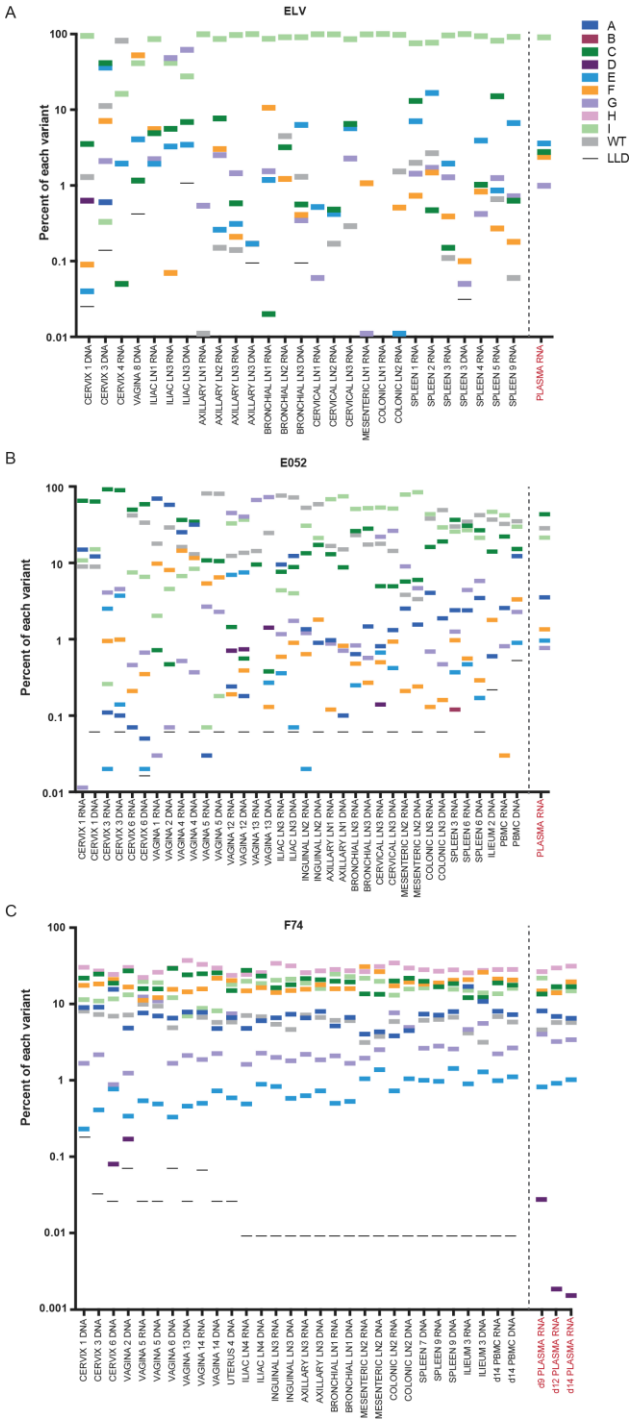

Fig. S7. Proportion of individual variants using NGS. The proportion of each variant was determined in a subset of SIV positive tissues, cells and plasma from ELV necropsied at day 6 (A), E052 necropsied at day 7 (B), and F74 necropsied at day 14 (C). Rectangular symbols are used for each variant (A-WT). The lower limit of detection is indicated with a black line if above 0.01%. All other samples had lower limit of detection of less than 0.01%.

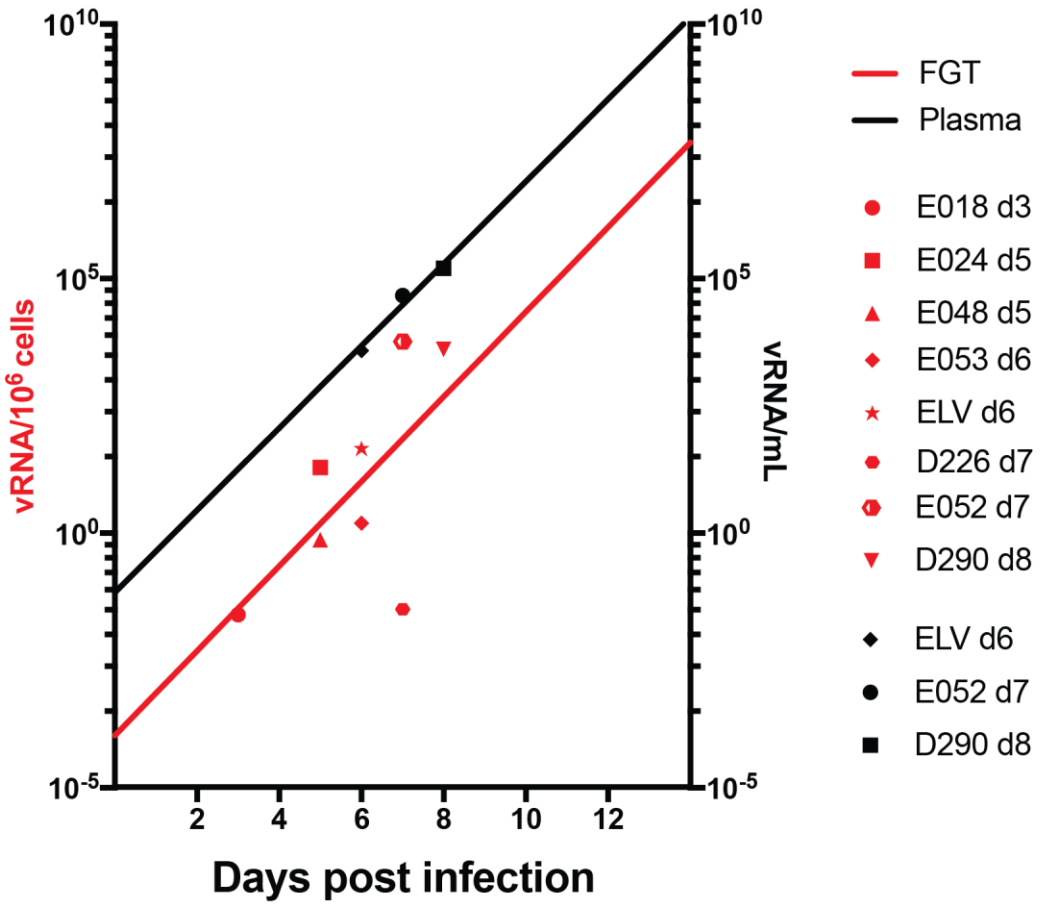

Fig. S8. Growth rates during FGT and systemic viral replication. The level of vRNA copies in SIV+ tissue pieces of the FGT was measured at necropsy in 8 animals (3-8dpi; red symbols) and the average growth rate across all animals was estimated (red line). Similarly, average growth rate of plasma virus was also estimated in 3 viremic animals (6-8 dpi; black lines and black symbols).

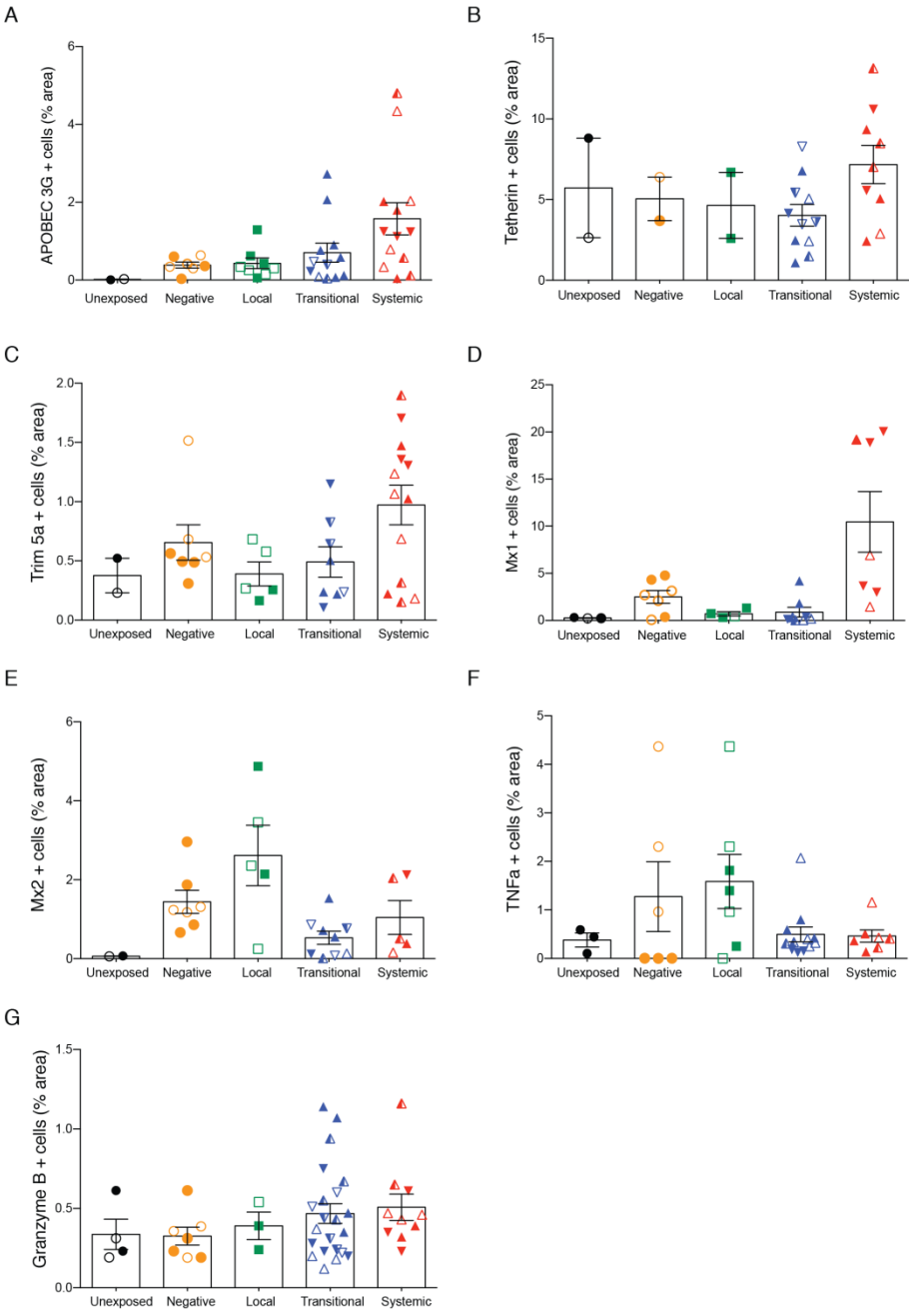

Fig. S9. No significant difference in the local expression of many proinflammatory and AVFs. Quantitative image analysis was used to assess expression levels of APOBEC3G (A), Tetherin (B), TRIM5α (C), Mx1 (D), Mx2 (E), TNFα (F), and Granzyme B (G) in the FGT. While there were trends toward enrichment of some antiviral factors as infection progressed, none of these factors were significantly upregulated during primary infection. Each symbol represents a unique animal and when multiple tissues per animals were analyzed, replicate symbols are shown.

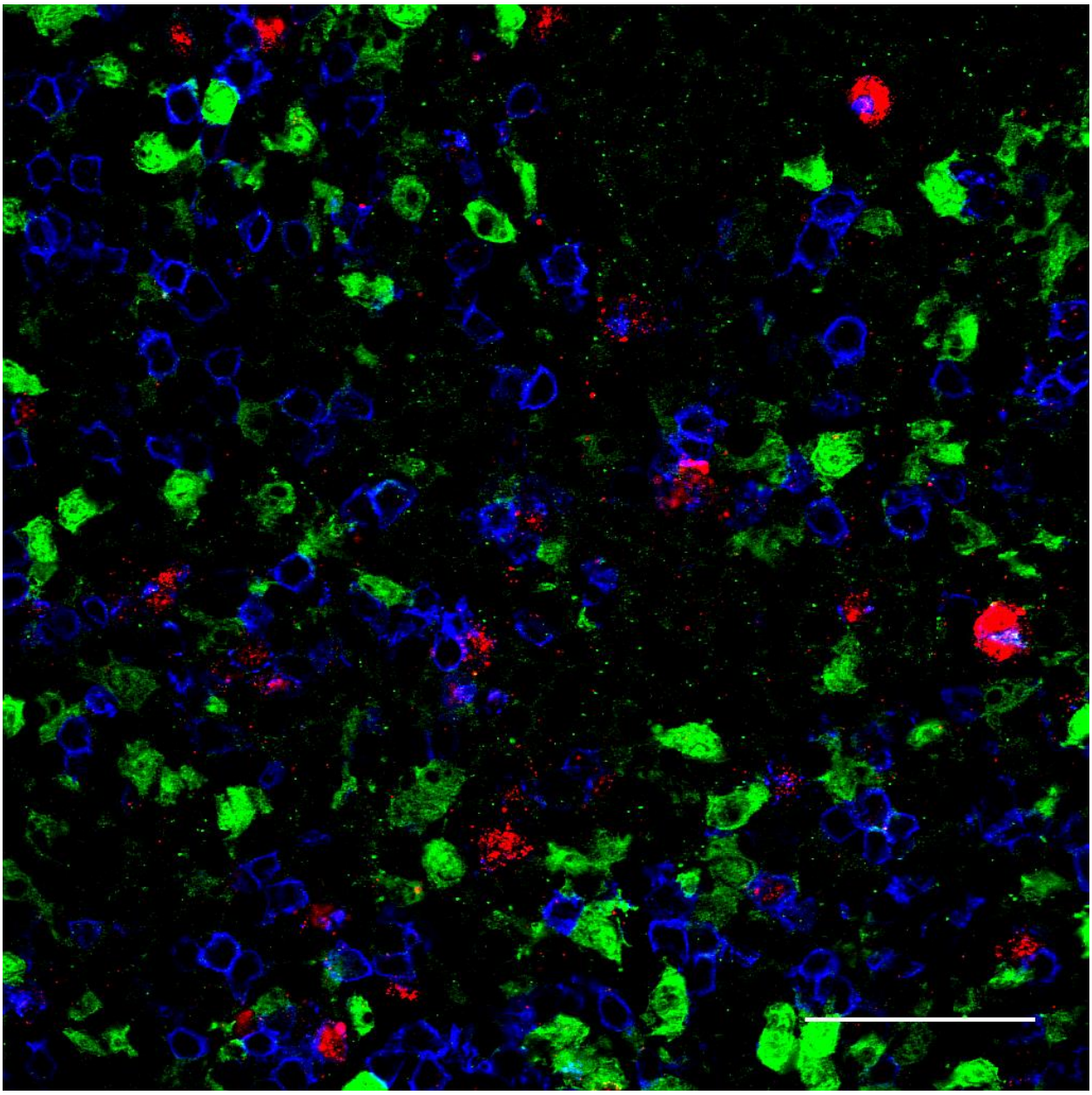

Fig. S10. AVFs measured in SIV-positive and SIV-negative cells. The relative expression levels of the antiviral factors Mx2, APOBEC3G, Tetherin, and TRIM5α were quantified together in SIV negative or SIV^+ $CD4^+$ cells using fluorescent confocal microscopy. CD4 staining in blue, vRNA in red, and antiviral factors in green. Representative image shown. Scale bar equals 100μm.